

## Dynamical Feedbacks of the Southern Annular Mode in Winter and Summer

ELIZABETH A. BARNES AND DENNIS L. HARTMANN

*Department of Atmospheric Sciences, University of Washington, Seattle, Washington*

(Manuscript received 18 November 2009, in final form 11 February 2010)

### ABSTRACT

The persistence of the southern annular mode (SAM) is studied during austral winter (June–September) and summer (December–March) using observations of the three-dimensional vorticity budget. Analysis of the relative vorticity tendency equation shows that convergence of eddy vorticity flux in the upper troposphere, coupled with a secondary circulation, constitutes a positive eddy feedback that acts to sustain the vorticity anomaly associated with the jet shift against drag. The feedback exhibits a strong seasonality, with summer months revealing a positive feedback through much of the hemisphere and winter months showing a positive feedback over the Indian Ocean but not over the western Pacific. Results suggest that the lack of wintertime feedback over the western Pacific is due to the weakness of the eddy-driven midlatitude jet in that region.

### 1. Introduction

The southern annular mode (SAM) is the leading mode of variability of the Southern Hemisphere tropospheric winds and is often described as a zonally symmetric north–south shift of the midlatitude jet (Hartmann and Lo 1998; Thompson and Wallace 2000; Lorenz and Hartmann 2001; Yang and Chang 2007). The SAM is an internal mode of variability in the Southern Hemisphere, and understanding the mechanisms that sustain the SAM anomalies will aid models in reproducing the real atmosphere and provide an opportunity for seasonal forecasting. In terms of climate change projections, it is important that we understand the internal modes of variability and their sustaining mechanisms, given that in the presence of feedbacks, a small external forcing that projects onto an internal mode can cause large changes in the variability of the atmosphere.

In the zonal mean, Lorenz and Hartmann (2001) showed that the persistence of this annular mode was extended because of a positive feedback between the SAM zonal wind anomalies and the eddy momentum fluxes. Multiple studies have suggested that the positive feedback between the eddies and the low-frequency flow sustains the low-frequency anomalies against surface drag (Feldstein

and Lee 1998; Robinson 2000; Gerber and Vallis 2007; Hartmann 2007; Barnes and Hartmann 2010, hereafter BH10). Robinson (1996, 2000) demonstrated the importance of surface drag by showing that when the jet shifts poleward, the eddy fluxes produce a poleward transport of heat that typically reduces the baroclinicity in the region of the shifted jet (and thus restricts the production of more eddies). In the presence of drag, the poleward transport of heat, and thus the destruction of the temperature gradient, is balanced by the adiabatic cooling from a thermally indirect Ferrel cell, which moves momentum supplied by eddy fluxes at upper levels to the surface (Hartmann and Lo 1998; Robinson 2006; Hartmann 2007).

Throughout the winter, the upper troposphere of the Southern Hemisphere exhibits a double jet structure, with a strong subtropical jet near 30°S and an eddy-driven jet centered near 50°S over the Indian Ocean that weakens and turns poleward to 60°S over the Pacific, described as the “spiral jet” by Williams et al. (2007). Although the exact latitude of the eddy-driven jet varies with longitude and season, we will call it the “midlatitude jet” throughout this paper. Many studies have documented the seasonality of the Southern Hemisphere jets and have found that the midlatitude jet is present over the Indian Ocean throughout the year. The subtropical jet is the dominant upper-tropospheric jet during the winter but is severely diminished during the summer months (Bals-Elsholz et al. 2001; Nakamura and Shimpō 2004; Hoskins and Hodges 2005). Over the North Pacific Ocean, Eichelberger and Hartmann (2007) found that

---

*Corresponding author address:* Elizabeth A. Barnes, Department of Atmospheric Sciences, University of Washington, Box 351640, Seattle, WA 98195.  
E-mail: eabarnes@atmos.washington.edu

the eddy feedback is most suppressed when the subtropical and midlatitude jets fuse into one strong subtropical jet. They suggested that the feedbacks are weakened when the subtropical jet becomes dominant and acts as a strong waveguide, inhibiting the meridional propagation of the waves required for a positive feedback. Nakamura and Shimpō (2004) confirmed that the subtropical jet acts as a waveguide for synoptic-scale eddies, although this jet is not favorable for their growth.

Previous studies of eddy feedbacks associated with meridional shifts of midlatitude jets have focused solely on the zonal-mean zonal momentum equation (Lorenz and Hartmann 2001, 2003; Codron 2005, 2007; Eichelberger and Hartmann 2007). Recently, BH10 introduced a three-dimensional vorticity-budget framework to study feedbacks in a local domain without taking the zonal mean. Using this technique, they showed that a meridional shift of the midlatitude jet over the North Atlantic Ocean during winter, referred to as the North Atlantic Oscillation (NAO), experiences a positive eddy feedback that extends the NAO's persistence. A novelty of using the relative vorticity equation is that one does not have to take the zonal mean; thus it becomes possible to study zonal asymmetries in the interactions between the low-frequency flow and the eddies. In this paper, we apply the method of BH10 to the Southern Hemisphere with the primary goal of demonstrating quantitatively that the net eddy transport of vorticity constitutes a positive feedback and that its strength is both regionally and seasonally dependent.

## 2. Data

The dataset consists of 44 years (1958–2001) of  $2.5^\circ \times 2.5^\circ$  latitude–longitude gridded daily (1200 UTC) sea level pressure (SLP), zonal velocity  $u$ , meridional velocity  $v$ , and the vertical component of relative vorticity  $\zeta$  [ $=\nabla \times \mathbf{u}$ , where  $\mathbf{u} = (u, v)$ ] on 12 vertical levels (1000, 925, 850, 775, 700, 600, 500, 400, 300, 250, 200, and 150 mb) from the 40-yr European Centre for Medium-Range Weather Forecasts (ECMWF) Re-Analysis (ERA-40) (Uppala et al. 2005). Only Southern Hemisphere fields are analyzed in this paper, and we note that these data are based on limited observations for the first part of the record. We performed the analysis on data from the 1970–2001 period only (not shown) and obtained nearly identical results. When appropriate, the 44-yr dataset is split into austral winter [June–September (JJAS)] and summer [December–March (DJFM)] months and the time series analysis is applied to each 121-day season (ignoring 31 March during leap years). To aid in visualization, we have filtered the plots of spatial fields by expanding in spherical harmonics and truncating at T25.

To analyze the variability of the atmosphere, we define daily anomaly data throughout this paper by removing the mean seasonal cycle. The mean seasonal cycle is a smooth curve computed as the annual mean plus the first four Fourier harmonics of the daily climatology for all seasons over the 44 years of data. Thus, the magnitude of a variable  $x$  at a single location can be decomposed into a climatological value  $\bar{x}$  plus an anomalous value  $\hat{x}$  such that  $x = \bar{x} + \hat{x}$ . Part of this analysis requires splitting the anomalous fields into high- and low-frequency components, representing variability on time scales less than and greater than 7 days, respectively. This frequency division uses a 7-day cutoff Lanczos filter with 41 weights (Hamming 1989) applied to all seasons over the 44 years. The winter and summer fields were retained after frequency filtering was performed on all months of the dataset.

## 3. Southern annular mode

Various definitions of the SAM include empirical orthogonal function (EOF) analysis of the 500-, 300-, or 1000-mb geopotential heights, zonally averaged zonal wind, or sea level pressure field (Hartmann and Lo 1998; Thompson and Wallace 2000; Lorenz and Hartmann 2001; Sen Gupta and England 2007). We define the SAM as the leading EOF of the monthly-mean sea level pressure anomalies throughout the Southern Hemisphere (equator to pole) for all months of the year. Before performing EOF analysis, the data were properly weighted to account for the decrease in area toward the pole. The SAM pattern explains 18% of the month-to-month variance of sea level pressure over the hemisphere and is distinct from the other eigenvectors according to the criterion outlined by North et al. (1982).

The following results use a SAM index  $Z(t)$  defined by projecting daily sea level pressure anomalies onto the SAM pattern of the monthly-mean sea level pressure. Here  $Z$  is normalized to have a standard deviation of one and a mean of zero by construction. We analyze the summer and winter seasons separately using  $Z$  derived from the annual EOF; note, however, that results are nearly identical (time series correlated at 0.99) if seasonal EOFs are used to define seasonal indices instead.

SAM patterns in fields other than sea level pressure are obtained by regressing  $Z$  onto the daily anomaly maps. We present the summer and winter SAM patterns of anomalous 300-mb zonal wind associated with a one standard deviation variation of  $Z$  alongside the seasonal mean zonal wind in Fig. 1. The summer SAM pattern (Fig. 1a) depicts a nearly zonal north–south shift of midlatitude jet. The wintertime pattern differs substantially (Fig. 1b). During the winter months, a strong subtropical jet forms and

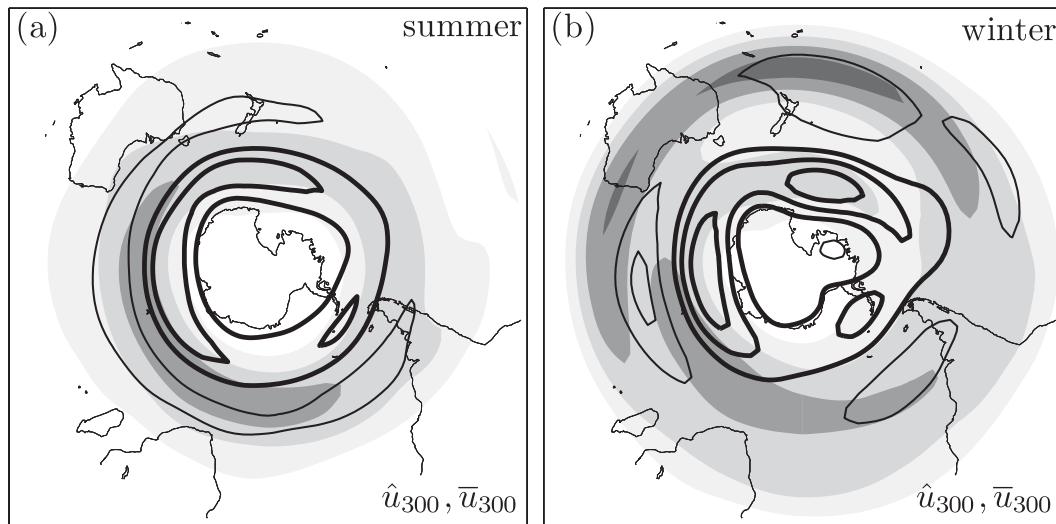


FIG. 1. Anomalous 300-mb zonal wind associated with the SAM defined as the leading EOF of monthly-mean sea level pressure during (a) summer and (b) winter. Contours are drawn every  $1.75 \text{ m s}^{-1}$  with positive contours denoted by thick black contour lines and negative contours as thin contour lines. The zero contour has been omitted. Shading denotes the seasonal-mean zonal wind contoured every  $10 \text{ m s}^{-1}$ .

extends from the Indian Ocean into the mid-Pacific, with its maximum occurring over the western Pacific. Figure 1b depicts the midlatitude jet weakening over the Pacific and eastern Indian Ocean and a localized region of zonal winds turning slightly poleward, abruptly ending over the mid-Pacific. Nakamura and Shimpo (2004) show that during the summer season, the upper-level high-frequency eddy variability is strong throughout the hemisphere, but in winter the eddy variability is weak over the Pacific, consistent with the lack of an eddy-driven jet in the region. During the winter, the SAM anomalies describe a meridional shift of the eddy-driven midlatitude jet over the Indian Ocean, but over the western Pacific the SAM pattern describes a strengthening/weakening (pulsing) of the localized region of westerlies near  $60^{\circ}\text{S}$  and a weak pulsing of the subtropical jet (Aoki et al. 1996; Bals-Elsholz et al. 2001; Lee and Kim 2003; Codron 2005; Yang and Chang 2006; Codron 2007).

Previous studies have shown that variability associated with a meridional shift of the eddy-driven jet exhibits an eddy feedback while a pulsing does not (Lorenz and Hartmann 2001, 2003; Eichelberger and Hartmann 2007). In addition, Eichelberger and Hartmann (2007) argue that the subtropical jet is driven by the Hadley circulation and its variability lacks an eddy feedback because it inhibits the meridional propagation of the eddies. Figure 1b shows that over the Pacific during winter, a strong, elongated climatological midlatitude jet is absent and the subtropical jet dominates, with the SAM describing a pulsing of the westerlies. Thus, one might expect a lack of eddy feedback during winter over the Pacific Ocean basin. During the summer (Fig. 1a), the SAM describes a

meridional shifting of the midlatitude jet throughout most of the hemisphere, and thus one would expect to find a positive eddy feedback where the eddy-driven jet is strong. Figure 2 shows the autocorrelation functions of the SAM index for the winter and summer months. In support of a reduced feedback, the winter SAM index has a shorter decorrelation time when compared to that of the summer season, which we will suggest is associated with a lack of feedback sustaining the anomaly. Figure 2 also shows the autocorrelation of a “split-jet” index (SJI), which defines a strengthening and weakening of the zonal wind over the Pacific Ocean. This index will be discussed in section 7.

The seasonal SAM variability of the midlatitude jet is also evident in the mass-weighted upper-level (300–150 mb) and lower-level (1000–850 mb) relative vorticity fields displayed in Fig. 3. The high-phase SAM denotes an anomalous increase in cyclonic vorticity near the pole,  $90^{\circ}$  out of phase with the shift in upper-level zonal wind. The boxed domains in Fig. 3 define the Indo-Atlantic sector as the domain poleward of  $30^{\circ}\text{S}$ , between  $60^{\circ}\text{W}$  and  $120^{\circ}\text{E}$ , and the Pacific sector as the domain poleward of  $30^{\circ}\text{S}$ , between  $120^{\circ}\text{E}$  and  $60^{\circ}\text{W}$ . We define the Southern Hemisphere region to be the entire cap extending poleward of  $30^{\circ}$ , thus encompassing the Indo-Atlantic and Pacific sectors. Results are not sensitive to the exact meridional or zonal extents of these sectors.

At this point, a brief discussion on the “annular” nature of the SAM is warranted. Previous studies have shown that multiple definitions of the SAM possess coherent annular features (Cohen and Saito 2002; Watterson 2007). We have calculated the time series of the SAM

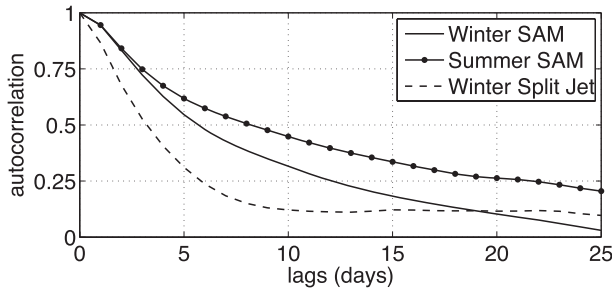


FIG. 2. Autocorrelations of the seasonal SAM indices and the split-jet index.

over the Indo-Atlantic and Pacific regions by projecting the SAM’s sea level pressure pattern onto the two domains separately. We find that during the summer, the Indo-Atlantic and the Pacific SAM patterns are correlated at 0.73, while they are correlated at 0.56 during the winter. Not surprisingly, winter has the least zonally symmetric SAM pattern and is also the season with the least amount of temporal correlation between the two regions.

The results thus far suggest that the underlying dynamics of the SAM during the summer and winter seasons are different and that the seasonality of the persistence of the SAM may be due to the zonal asymmetry resulting from the absence of a shifting midlatitude jet over the Pacific during winter. Here, we investigate these seasonal and spatial differences in the eddy feedbacks associated with the SAM.

#### 4. Vorticity budget and feedback mechanism

##### a. Budget

This study utilizes the relative vorticity equation. This diagnostic is chosen because relative vorticity is a scalar quantity with budget terms that are straightforward to interpret in the context of large-scale dynamics. The relative vorticity tendency at a given horizontal location and vertical pressure level is given by (Holton 2004)

$$\frac{\partial \zeta}{\partial t} = -\nabla \cdot [(\zeta + f)\mathbf{u}] - \omega \frac{\partial \zeta}{\partial p} + \hat{\mathbf{k}} \cdot \left( \frac{\partial \mathbf{u}}{\partial p} \times \nabla \omega \right) + \mathcal{F}, \tag{1}$$

where  $\nabla \cdot$  and  $\nabla$  respectively denote the 2D horizontal divergence and gradient,  $f$  is the Coriolis parameter,  $\omega$  is the vertical velocity,  $\hat{\mathbf{k}}$  is the vertical unit vector, and  $\mathcal{F}$  is the forcing due to friction. One can ignore the vertical advection of vorticity and the tilting terms (second and third right-hand terms) in (1) using simple scaling arguments (Holton 2004). We can split the terms into mean and anomalous quantities and rearrange to obtain an equation for the vorticity tendency as done in BH10:

$$\begin{aligned} \frac{\partial \hat{\zeta}}{\partial t} = & [-\langle \bar{\zeta} + f \rangle \nabla \cdot \hat{\mathbf{u}} - \hat{\zeta} \nabla \cdot \bar{\mathbf{u}}]_{\text{stretching}} \\ & + [-\nabla \cdot (\hat{\zeta} \hat{\mathbf{u}})]_{\text{eddy}} + [-\hat{\mathbf{u}} \cdot \nabla (\bar{\zeta} + f) - \bar{\mathbf{u}} \cdot \nabla \hat{\zeta}]_{\text{wave}} \\ & + \{-\nabla \cdot [\bar{\mathbf{u}}(\bar{\zeta} + f)]\}_{\text{clim}} + \mathcal{F}, \end{aligned} \tag{2}$$

where we have made the approximation that  $\partial \hat{\zeta} / \partial t \gg \partial \bar{\zeta} / \partial t$  (the climatological-mean vorticity tendency is not identically equal to zero because of its seasonal component).

The first bracketed term on the rhs of (2) is the vorticity source due to divergence, often referred to as the “stretching term.” The second rhs bracketed term represents the forcing of the anomalous vorticity by the divergence of the anomalous vorticity flux and will be termed the “eddy forcing.” The third bracketed term of (2) is the linear wave term, composed of the advection of the background vorticity by the anomalous wind and the advection of the anomalous vorticity by the mean wind. The fourth bracketed term is composed of seasonal-mean quantities and represents the climatological vorticity flux convergence (stationary wave forcing), which is nearly constant throughout the winter season.

##### b. Feedback mechanism

We envision a feedback mechanism that compensates for the effect of surface drag and enables persistence and self-maintenance of the SAM pattern. This mechanism is the same as that presented in BH10 with regard to the NAO. It is important to stress that this mechanism is similar to those described in zonal-mean frameworks by previous authors (Robinson 2000, 2006; Gerber and Vallis 2007; Hartmann 2007). We briefly describe the mechanism here and refer readers to BH10 for more details and a schematic of the mechanism (BH10; Fig. 3).

The midlatitude jet in the Southern Hemisphere is a source of eddies and we expect that a meridional shift of the jet is coupled to a similar shift in the eddy source region (Hartmann 2007). If the eddies propagate away from the jet before breaking, there will be a convergence of eddy vorticity flux at upper levels, which reinforces the jet in its shifted position. Upper-level divergence balances the convergence of eddy vorticity flux through the stretching term in (2), which requires mass convergence at the surface. This mass convergence generates vorticity and maintains the shifted jet against surface friction. The feedback loop is completed by the fact that this secondary circulation produces adiabatic heating and cooling in such a way that the baroclinicity is maintained, sustaining a balanced jet and enhancing eddy growth in the region of the shifted jet. These new eddies will further reinforce the jet in its anomalous location via the mechanism described, thus creating a feedback that extends the persistence of the shifted jet.

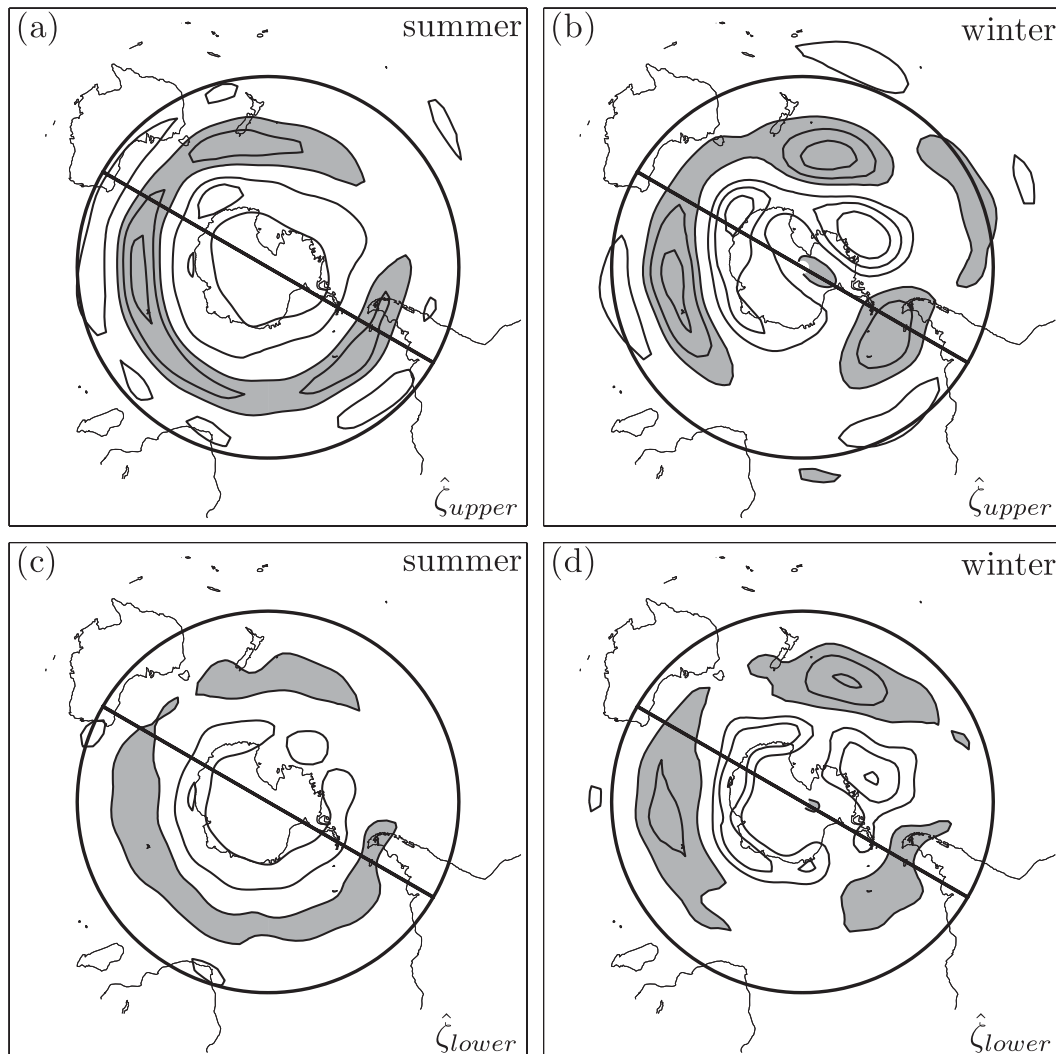


FIG. 3. SAM structures of the mass-weighted relative vorticity at (a),(b) upper levels and (c),(d) lower levels during (a),(c) summer and (b),(d) winter. Contours are drawn every  $2 \times 10^{-6} \text{ s}^{-1}$  for the upper levels and every  $1.5 \times 10^{-6} \text{ s}^{-1}$  for the lower levels, with positive contours shaded and the zero contour omitted. Also drawn are the regional definitions of the Indo-Atlantic and Pacific sectors used in the analysis.

## 5. Summer feedback analysis of the SAM

During the summer, the SAM manifests itself as a nearly zonally symmetric meridional shift of the midlatitude jet (Figs. 1a and 3a,c). In this section, we will show a nearly zonally symmetric feedback between the eddies and the vorticity anomalies that extends the persistence of the SAM during summer.

### a. Summer forcing patterns

The analysis described uses mass-weighted upper- and lower-level fields, averaged for the 300–150- and 1000–850-mb levels, respectively. The results are robust in that the pairing of any upper-level forcing field and any

lower-level vorticity field produces similar conclusions (not shown). Figure 4 shows the patterns obtained when  $Z$  is regressed onto the summer forcing fields on the rhs of (2). The stretching field organizes in an annular pattern with positive forcing around the coast of Antarctica and negative forcing equatorward (Fig. 4a). This pattern counters the positive forcing by the convergence of eddy vorticity flux, consistent with the proposed feedback mechanism (Fig. 4c). The linear wave forcing pattern associated with the summertime SAM shown in Fig. 4b has little organization and, as we will show, projects poorly onto the SAM vorticity anomaly pattern. It is possible to plot lagged-regression patterns of all four of these fields, and this has been done (not shown). The lagged patterns

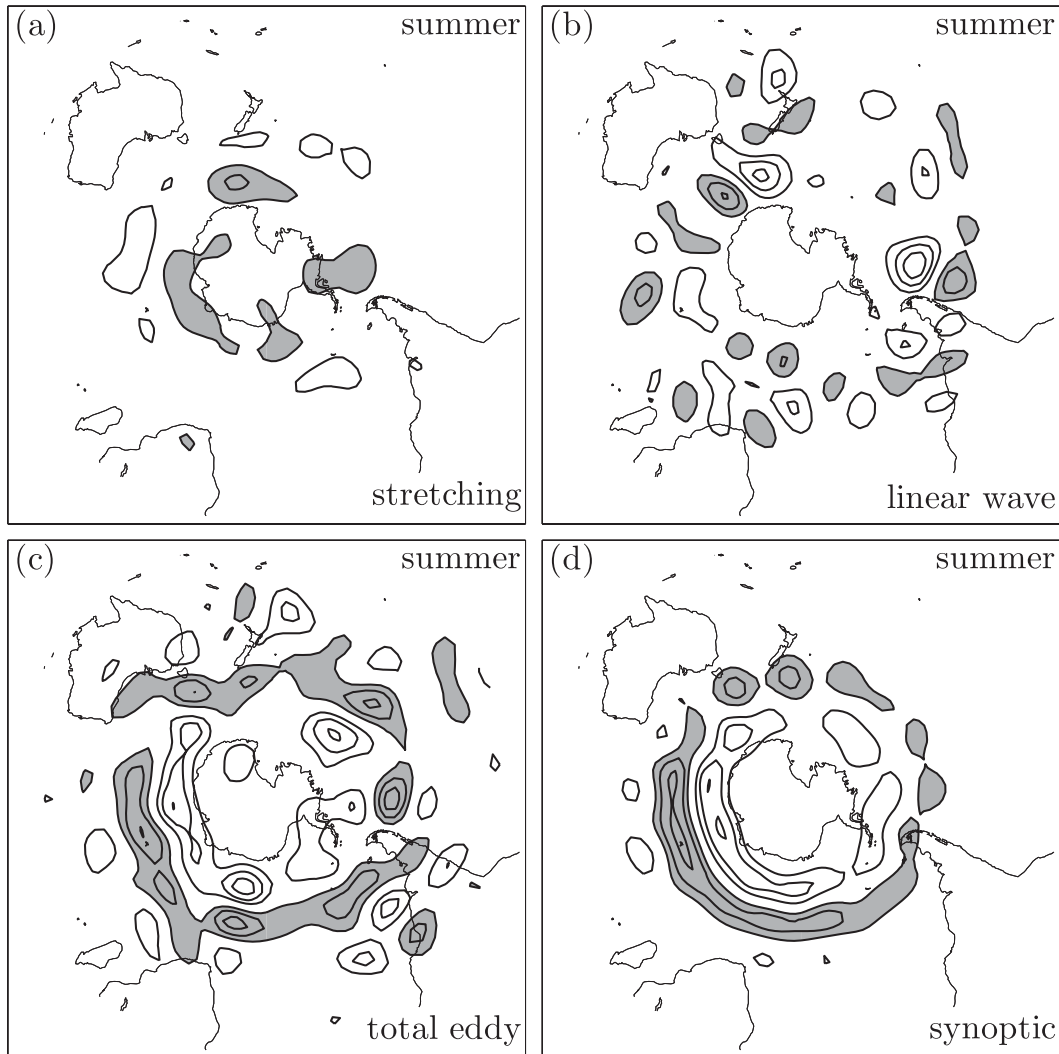


FIG. 4. Summer SAM structures of the upper-level (a) stretching term, (b) linear wave term, (c) total eddy forcing, and (d) synoptic eddy forcing obtained by regressing  $Z(t)$  onto the field. Contours are drawn every  $1.5 \times 10^{-11} \text{ s}^{-2}$  for (a),(b) and every  $8.75 \times 10^{-12} \text{ s}^{-2}$  for (c),(d), with positive contours shaded and the zero contour omitted.

appear similar to those shown in Fig. 4 for small positive and negative lags. This relationship will be quantified using time series analysis in the next section.

BH10 demonstrated that the high-frequency eddies were responsible for maintaining the NAO vorticity anomalies. Similarly, other studies have shown the importance of high-frequency eddies in driving and maintaining large-scale variability in the atmosphere (Nakamura and Wallace 1990; Branstator 1992; Lorenz and Hartmann 2001; Feldstein 2003; Eichelberger and Hartmann 2007). As done in BH10, we separate the “synoptic” (high-frequency) eddy forcing from the total forcing by high-pass filtering ( $<7$  days) the anomalous horizontal winds  $\mathbf{u}'$  and the anomalous vorticity  $\zeta'$  and computing the component of the eddy forcing due to fluctuations on these synoptic time scales  $[-\nabla \cdot (\zeta' \mathbf{u}')]$ . The resulting regression

(Fig. 4d) of the summertime  $Z$  onto the synoptic eddy forcing aligns well with the SAM vorticity structure (Figs. 3a,c), supporting the hypothesis that the synoptic eddies are acting to sustain the large-scale SAM structure. We quantify this result in the next section.

#### b. Summer time series analysis

The technique employed here is similar to that of BH10 although it has been simplified since results are robust to the specific method chosen. We define the eddy forcing time series  $M$  by the projection of the daily eddy-forcing field onto the SAM’s lower-level anomalous vorticity pattern, normalized for unit variance. Hence,  $M$  indicates how well the upper-level forcing pattern aligns with the lower-level vorticity anomaly, or to what extent the upper-level eddy forcing sustains the anomaly against friction. By

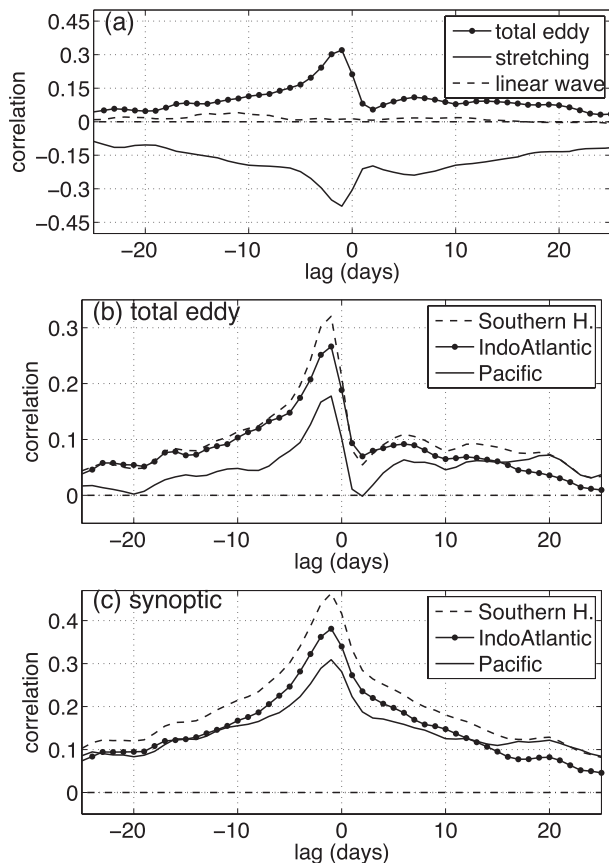


FIG. 5. (a) Summer cross correlations between  $Z$  and  $M$  in the SH region for the total eddy forcing (circles), stretching term forcing (solid), and linear wave forcing (dashed). (b) Summer cross correlations between  $Z$  and  $M$  in the entire SH (dashed), Indo-Atlantic (circles), and Pacific (solid) sectors. (c) Summer cross correlations between  $Z$  and the synoptic eddy forcing in three domains. In all panels, positive lags imply that  $Z$  leads  $M$ .

defining  $M$  in this way, we have implicitly assumed that the optimal shape of the eddy field for forcing the SAM anomaly is the shape of the SAM vorticity anomaly itself. BH10 presents a heuristic argument suggesting why this may be appropriate for a steady Rossby wave.

We hypothesize that a positive feedback requires the upper-level eddy forcing to sustain the lower-level SAM vorticity anomaly. This implies that

$$\frac{dZ}{dt} = M - \frac{Z}{\tau}, \quad (3)$$

where  $\tau$  is the decay time scale and  $M$  is composed of both a random forcing component and a component organized by the low-frequency vorticity anomalies. Equation (3) is a simple stochastic index model that has been used in many studies to model fluctuations of zonal jets (Robinson 1994; Kidson and Watterson 1999; Watterson 2000; Lorenz and Hartmann 2001).

Figure 5a shows the cross correlations between  $M$  and  $Z$  for the Southern Hemisphere domain during the summer, with positive lags signifying that the SAM leads the eddy forcing. These cross correlations measure how well the forcing patterns (i.e., Fig. 4) project onto the NAO vorticity pattern at various lags. The greatest correlations occur at negative lags, consistent with the low-frequency anomalies being driven primarily by random fluctuations of the eddies as described by (3). Positive correlations at positive lags larger than the period of a typical synoptic disturbance (7 days) imply a positive feedback between the eddy forcing and the slowly varying vorticity field. The total eddy forcing time series is positively correlated with  $Z$  at the 95% confidence level for positive lags 0 to +25 days and beyond (see appendix A of BH10 for details on how this significance level was calculated). Although the cross correlations are small, they are consistently positive over a long period of time and thus have a significant effect on the persistence of the jet shifts, increasing the  $e$ -folding time of the summer SAM from 4.5 to 13 days, as determined by spectral analysis (results not shown; see BH10 for method). These positive correlations support the hypothesis that the SAM anomalies organize the eddy fluxes for self-maintenance throughout the entire Southern Hemisphere during summer. As hypothesized, the stretching term exhibits a negative correlation with  $Z$ , implying that the stretching field projects negatively onto the SAM vorticity anomaly, thus acting to balance the total eddy forcing at upper levels (Fig. 5a). The linear wave term has near-zero correlations at all lags because of its unorganized structure, as was seen in Fig. 4b.

Figure 5b compares the cross correlations between  $Z$  and  $M$  defined in the Southern Hemisphere, Indo-Atlantic, and Pacific sectors during summer. The cross correlations in the Indo-Atlantic are significant at the 95% confidence level for lags 0 to +21 days and those in Pacific are significant for lags 0 to +25 days and beyond. From this figure, we can see that an organized feedback between the eddies and the SAM structure is found equally in the two sectors and is indicative of the feedback throughout the entire hemisphere. The correlations of the synoptic eddy forcing and  $Z$  are plotted in Fig. 5c and confirm that the positive correlations at positive lags are associated with the high-frequency eddies and their organization by the low-frequency flow. Hence, the high-frequency eddies drive the net positive feedback between the eddies and the SAM structure throughout the Southern Hemisphere domain.

## 6. Winter feedback analysis of the SAM

Here, we apply the same analysis done for the summer to the winter fields associated with the SAM. As previously noted, past work has demonstrated that the structure of

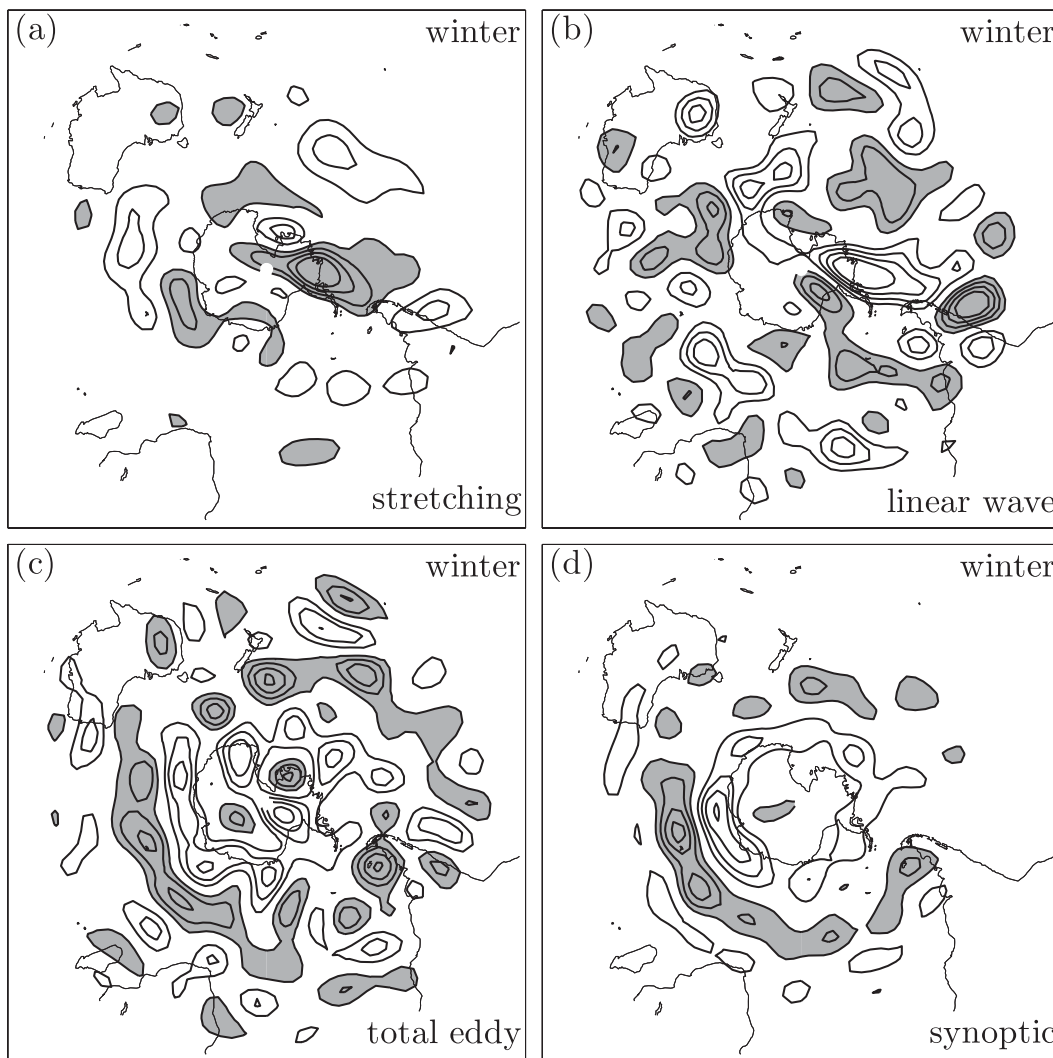


FIG. 6. As in Fig. 4, but for winter SAM structures.

the SAM during winter is less zonally symmetric than its summertime manifestation. The following results support a zonally asymmetric eddy feedback as well.

*a. Winter forcing patterns*

Figure 6 displays the regression patterns of the SAM vorticity forcing fields during winter. Unlike during the summer season, the wintertime total eddy and synoptic forcing patterns (Figs. 6c,d) only align with the SAM vorticity anomaly in the Indo-Atlantic sector (Figs. 3b,d), while the fields appear less organized over the Pacific. Similarly, the stretching pattern is opposite in sign to the SAM vorticity anomaly in the Indo-Atlantic sector only (Fig. 6a), although it is most organized over the eastern Indian Ocean. The linear wave forcing plotted in Fig. 6b appears noisy and unorganized, similar to the summer structure, although larger in magnitude. Again, it is possible to plot

lagged-regression patterns of all four of these fields, and this has been done for the winter as well (not shown). The lagged patterns appear similar to those shown in Fig. 6 for small positive and negative lags.

*b. Winter time series analysis*

Figure 7a shows the cross correlations between  $M$  and  $Z$  for the Southern Hemisphere domain during the winter, with positive lags signifying that the SAM leads the eddy forcing. As during summer, the entire Southern Hemisphere exhibits positive correlations at large positive lags between the eddies and the SAM, implying an eddy feedback. In addition, the stretching term offsets the effects of the eddies in a similar manner. Unlike during the summer, the linear wave term projects positively onto the SAM vorticity anomaly at small negative lags and negatively at small positive lags, indicative of a propagating wave.

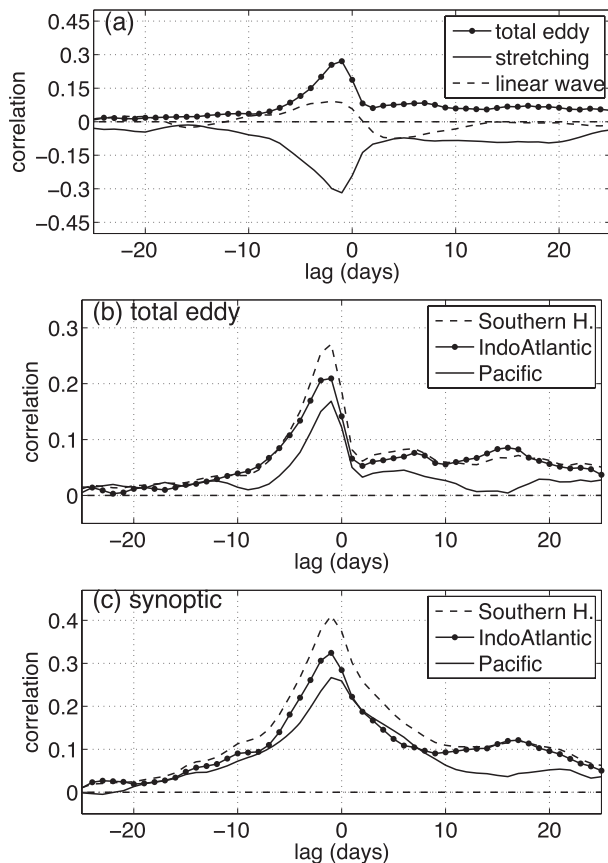


FIG. 7. As in Fig. 5, but for winter cross correlations.

We plot the total eddy forcing correlations with  $Z$  for the three domains during austral winter in Fig. 7b. Comparing with those for the summer (Fig. 5b), we see a striking difference. Although a positive feedback exists in the Indo-Atlantic sector during both seasons, a strong feedback is absent over the Pacific during winter. Consistent with this observation, we find that most of the wintertime feedback in the Southern Hemisphere domain is due to the feedback in the Indo-Atlantic sector alone. In Fig. 7b, the correlations in the Pacific are statistically different from zero for lags 0 to +10 days, while the correlations in the Indo-Atlantic are statistically different from zero for lags 0 to +25 days and beyond. Cross correlations of the wintertime synoptic eddy forcing show that the high-frequency eddy forcing contributes to the difference in eddy feedback between the two sectors (Fig. 6c).

Previous studies have demonstrated that the wintertime SAM manifests itself as a pulsing of zonal winds in the western Pacific, rather than a meridional shifting of an elongated eddy-driven midlatitude jet (as in the Indian Ocean basin) (Aoki et al. 1996; Bals-Elsholz et al. 2001; Lee and Kim 2003; Yang and Chang 2006; Codron 2007). Based on this work, we apply the previous correlation analysis to localized western Pacific ( $30^{\circ}$ – $90^{\circ}$ S,

$135^{\circ}$ E– $135^{\circ}$ W) and Indian Ocean ( $30^{\circ}$ – $90^{\circ}$ S,  $45^{\circ}$ – $135^{\circ}$ E) domains to investigate the feedbacks in these contrasting regions. The resulting cross correlations (not shown) are similar to those in Fig. 7b, with correlations in the western Pacific dropping to zero by lag +10 days and the correlations in the Indian Ocean staying positive beyond +25 days. In addition, areas outside of these two regions have negligible correlations, consistent with the weaker SAM signal there. We conclude that the difference in feedback between the Indo-Atlantic and Pacific sectors results from a difference in feedback in the localized areas of the Indian Ocean and western Pacific. We suggest that this difference is due to the lack of an eddy-driven midlatitude jet over the western Pacific. Consistent with previous studies, we find that the variability of the subtropical Hadley-driven jet does not exhibit a feedback.

## 7. Winter split jet

Yang and Chang (2006) studied the dynamics of the Southern Hemisphere split jet, a pulsing of the zonal wind in the wintertime western Pacific. In this section we use our methodology to test whether the split jet exhibits a positive eddy feedback. Our reasons are twofold: 1) to test our hypothesis that only meridional shifts of an eddy-driven midlatitude jet are sustained by a positive eddy feedback and 2) to demonstrate the importance of using lagged-correlation analysis when studying feedbacks.

Following Yang and Chang (2006), we define an SJI during winter as the difference in area-average 300-mb zonal wind anomalies over the two boxes shown in Fig. 8 (box A:  $55^{\circ}$ – $70^{\circ}$ S,  $150^{\circ}$ E– $150^{\circ}$ W and box B:  $35^{\circ}$ – $50^{\circ}$ S,  $150^{\circ}$ E– $150^{\circ}$ W)

$$\text{SJI} = \hat{U}_{300}^A - \hat{U}_{300}^B. \quad (4)$$

As in Yang and Chang (2006), we normalize the SJI to have a mean of zero and a variance of one. Composites of the 300-mb zonal wind during the top and bottom 5% SJI days are shown in Fig. 8. During a split-jet episode (positive SJI), two distinct regions of strong westerlies are seen in the western Pacific Ocean basin, associated with the subtropical jet and a localized region of strong zonal winds near Antarctica. In the unsplit-jet case (negative SJI), the strong westerlies near the pole are absent and only the subtropical jet is observed.

We now pose this question: Do eddies act to increase the persistence of split-jet events as defined during Southern Hemisphere winter? Here, the same time series analysis from previous sections is applied to the SJI in the western Pacific region ( $30^{\circ}$ – $90^{\circ}$ S,  $135^{\circ}$ E– $135^{\circ}$ W) since this is where the variability is greatest, although results are similar for the entire Pacific sector. The resulting cross

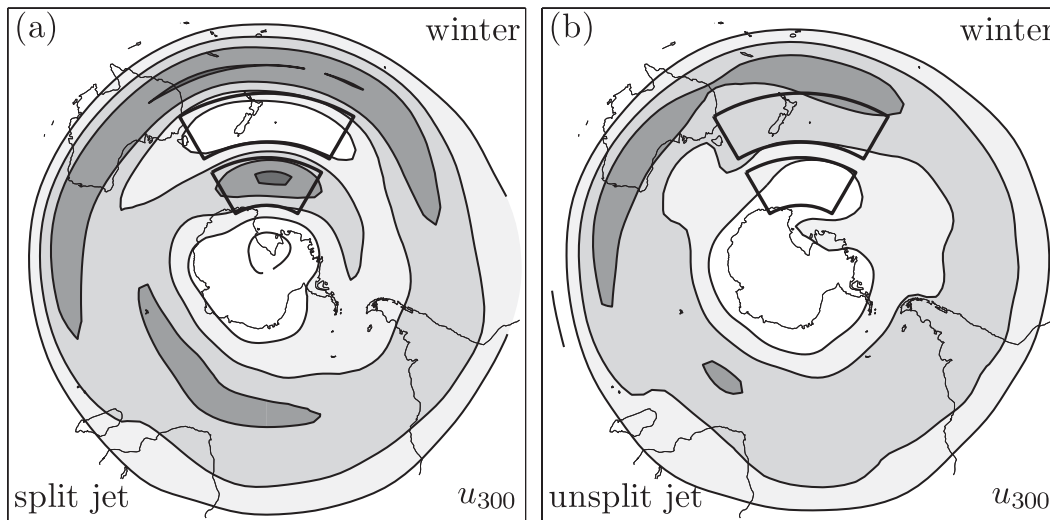


FIG. 8. 300-mb zonal wind associated with (a) a split jet and (b) an unsplit jet during winter. Contours are drawn every 10 m s<sup>-1</sup>; darker shading denotes more positive values and the zero contour is omitted.

correlations for the total eddy forcing are shown in Fig. 9. At large positive lags, the correlations of the SJI with the total eddy forcing are not statistically different from zero, implying that indeed no feedback exists between the eddies and the midlatitude jet in the western Pacific during split-jet episodes, consistent with our hypothesis.

Yang and Chang (2006) used simultaneous correlations to conclude that an eddy feedback is present during split-jet episodes. However, multiple studies have stressed that in the presence of damping, (3) implies that instantaneous (lag zero) composite analysis will always show some momentum forcing in phase with the wind anomalies whether or not a feedback is present (Lorenz and Hartmann 2001; Watterson 2002). Consistent with this, Fig. 9 shows that at a lag of zero days, the eddy forcing and the SJI are positively correlated at 0.1. However, we have demonstrated that no feedback between the split-jet variability and the eddies exists. Consistent with a lack of feedback, the SJI has a very short decorrelation time compared to the seasonal SAM indices, as shown in Fig. 2.

### 8. Discussion and concluding remarks

We applied the three-dimensional feedback analysis of BH10 to jet structures associated with the southern annular mode (SAM) to investigate spatial and seasonal differences in the strength of the eddy feedback. The main findings of this study are as follows:

- During austral summer, a positive feedback between the eddies and the jet anomalies extends the persistence of meridional shifts of the midlatitude eddy-driven jet.
- During austral winter, a positive feedback is concentrated over the Indian Ocean, where the midlatitude

jet is strong. Over the western Pacific Ocean, where the subtropical jet dominates, the low-frequency variability of the SAM manifests itself as a pulsing of a weak and localized midlatitude jet and an eddy feedback is absent.

The annular nature of the northern annular mode (NAM) has long been disputed, largely because of the zonal asymmetries introduced by the continents, while most studies have viewed the SAM in a zonally symmetric framework (Thompson and Wallace 1998, 2000; Ambaum et al. 2001; Lorenz and Hartmann 2001). We have demonstrated that during austral winter the dynamical mechanisms of the SAM are actually not zonally symmetric and conclude that eddy-feedback mechanisms previously diagnosed with zonal averages are really concentrated in regions where the midlatitude eddy-driven jet dominates.

These results suggest strong similarities between the wintertime variability of the midlatitude jet in the Southern and Northern Hemispheres. The meridional shifting of the

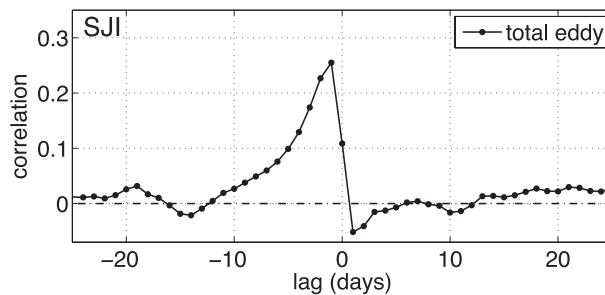


FIG. 9. Winter cross correlations between the split-jet index and the total eddy forcing in the western Pacific (30°–90°S, 135°E–135°W).

midlatitude eddy-driven jet over the Southern Hemisphere Indian Ocean basin can be likened to the North Atlantic Oscillation of the Northern Hemisphere, both showing a strong feedback between the low-frequency flow and the eddies (BH10). During winter, the midlatitude jet over the Southern Hemisphere's western Pacific Ocean is weak and the region is dominated by a strong subtropical jet, similar to the Northern Hemisphere Pacific Ocean basin. In both regions, the midlatitude jet variability is a pulsing rather than a shifting during annular mode episodes, and the eddy feedback is weak (Eichelberger and Hartmann 2007).

*Acknowledgments.* This work is supported by the Climate Dynamics Program of the National Science Foundation under Grant ATM 0409075.

#### REFERENCES

- Ambaum, M., B. Hoskins, and D. Stephenson, 2001: Arctic Oscillation or North Atlantic Oscillation? *J. Climate*, **14**, 3495–3507.
- Aoki, H., M. Shiotani, and I. Hirota, 1996: Interannual variability of the tropospheric circulation and its relation to the stratosphere in the Southern Hemisphere. *J. Meteor. Soc. Japan*, **74**, 509–523.
- Bals-Elsholz, T. M., E. H. Atallah, L. F. Bosart, T. A. Wasula, M. J. Cempa, and A. R. Lupo, 2001: The wintertime Southern Hemisphere split jet: Structure variability and evolution. *J. Climate*, **14**, 4191–4215.
- Barnes, E. A., and D. L. Hartmann, 2010: Dynamical feedbacks and the persistence of the NAO. *J. Atmos. Sci.*, **67**, 851–865.
- Branstator, G., 1992: The maintenance of low-frequency atmospheric anomalies. *J. Atmos. Sci.*, **49**, 1924–1946.
- Codron, F., 2005: Relation between annular modes and the mean state: Southern Hemisphere summer. *J. Climate*, **18**, 320–330.
- , 2007: Relations between annular modes and the mean state: Southern Hemisphere winter. *J. Atmos. Sci.*, **64**, 3328–3339.
- Cohen, J., and K. Saito, 2002: A test for annular modes. *J. Climate*, **15**, 2537–2546.
- Eichelberger, S. J., and D. L. Hartmann, 2007: Zonal jet structure and the leading mode of variability. *J. Climate*, **20**, 5149–5163.
- Feldstein, S. B., 2003: The dynamics of NAO teleconnection pattern growth and decay. *Quart. J. Roy. Meteor. Soc.*, **129**, 901–924.
- , and S. Lee, 1998: Is the atmospheric zonal index driven by an eddy feedback? *J. Atmos. Sci.*, **55**, 3077–3086.
- Gerber, E. P., and G. K. Vallis, 2007: Eddy–zonal flow interactions and the persistence of the zonal index. *J. Atmos. Sci.*, **64**, 3296–3311.
- Hamming, R. W., 1989: *Digital Filters*. Prentice Hall, 284 pp.
- Hartmann, D. L., 2007: The atmospheric general circulation and its variability. *J. Meteor. Soc. Japan*, **85B**, 123–143.
- , and F. Lo, 1998: Wave-driven zonal flow vacillation in the Southern Hemisphere. *J. Atmos. Sci.*, **55**, 1303–1315.
- Holton, J. R., 2004: *An Introduction to Dynamic Meteorology*. 4th ed. Elsevier, 535 pp.
- Hoskins, B. J., and K. I. Hodges, 2005: A new perspective on Southern Hemisphere storm tracks. *J. Climate*, **18**, 4108–4129.
- Kidson, J. W., and I. G. Watterson, 1999: The structure and predictability of the “high-latitude mode” in the CSIRO9 general circulation model. *J. Atmos. Sci.*, **56**, 3859–3873.
- Lee, S., and H.-K. Kim, 2003: The dynamical relationship between subtropical and eddy-driven jets. *J. Atmos. Sci.*, **60**, 1490–1503.
- Lorenz, D. J., and D. L. Hartmann, 2001: Eddy–zonal flow feedback in the Southern Hemisphere. *J. Atmos. Sci.*, **58**, 3312–3327.
- , and —, 2003: Eddy–zonal flow feedback in the Northern Hemisphere winter. *J. Climate*, **16**, 1212–1227.
- Nakamura, H., and J. M. Wallace, 1990: Observed changes in baroclinic wave activity during the life cycles of low-frequency circulation anomalies. *J. Atmos. Sci.*, **46**, 1100–1116.
- , and A. Shimpo, 2004: Seasonal variations in the Southern Hemisphere storm tracks and jet streams as revealed in a re-analysis dataset. *J. Climate*, **17**, 1828–1844.
- North, G. R., T. L. Bell, R. F. Cahalan, and F. J. Moeng, 1982: Sampling errors in the estimation of empirical orthogonal functions. *Mon. Wea. Rev.*, **110**, 699–706.
- Robinson, W. A., 1994: Eddy feedbacks on the zonal index and eddy–zonal flow interactions induced by zonal flow transience. *J. Atmos. Sci.*, **51**, 2553–2562.
- , 1996: Does eddy feedback sustain variability in the zonal index? *J. Atmos. Sci.*, **53**, 3556–3569.
- , 2000: A baroclinic mechanism for the eddy feedback on the zonal index. *J. Atmos. Sci.*, **57**, 415–422.
- , 2006: On the self-maintenance of midlatitude jets. *J. Atmos. Sci.*, **63**, 2109–2122.
- Sen Gupta, A., and M. H. England, 2007: Coupled ocean–atmosphere feedback in the southern annular mode. *J. Climate*, **20**, 3677–3692.
- Thompson, D. W., and J. M. Wallace, 1998: The Arctic Oscillation signature in the wintertime geopotential height and temperature fields. *Geophys. Res. Lett.*, **25**, 1297–1300.
- , and —, 2000: Annular modes in the extratropical circulation. Part I: Month-to-month variability. *J. Climate*, **13**, 1000–1016.
- Uppala, S. M., and Coauthors, 2005: The ERA-40 Re-Analysis. *Quart. J. Roy. Meteor. Soc.*, **131**, 2961–3012.
- Watterson, I. G., 2000: Southern midlatitude zonal wind vacillation and its interaction with the ocean in GCM simulations. *J. Climate*, **13**, 562–578.
- , 2002: Wave–mean flow feedback and the persistence of simulated zonal flow vacillation. *J. Atmos. Sci.*, **59**, 1274–1288.
- , 2007: Southern “annular modes” simulated by a climate model—Patterns, mechanisms, and uses. *J. Atmos. Sci.*, **64**, 3113–3131.
- Williams, L. N., S. Lee, and S.-W. Son, 2007: Dynamics of the Southern Hemisphere spiral jet. *J. Atmos. Sci.*, **64**, 548–563.
- Yang, X., and E. K. M. Chang, 2006: Variability of the Southern Hemisphere winter split flow—A case of two-way reinforcement between mean flow and eddy anomalies. *J. Atmos. Sci.*, **63**, 634–650.
- , and —, 2007: Eddy–zonal flow feedback in the Southern Hemisphere winter and summer. *J. Atmos. Sci.*, **64**, 3091–3112.